

Efficiency analysis of underground pumped storage hydropower plants

Javier Menéndez^{a,*}, Jesús M. Fernández-Oro^b, Mónica Galdo^b, Jorge Loredó^c

^a Hunaser Energy, 33005 Oviedo, Spain

^b Energy Department, University of Oviedo, 33271 Gijón, Spain

^c Mining Exploitation Department, University of Oviedo, 33004 Oviedo, Spain



ARTICLE INFO

Keywords:

Underground pumped-storage
Electricity storage
Energy efficiency
Variable renewable energies
Underground reservoir

ABSTRACT

Large-scale energy storage systems, such as underground pumped-storage hydropower (UPSH) plants, are required in the current energy transition to variable renewable energies to balance supply and demand of electricity. In this paper, a novel method to determinate the round trip energy efficiency in pumped storage hydropower plants with underground lower reservoir is presented. Two Francis pump-turbines with a power output of 124.9 and 214.7 MW (turbine) and a power input of 114.8 and 199.7 MW (pump), respectively, have been selected to investigate the overall operation of UPSH plants. Analytical models and two-phase 3D CFD numerical simulations have been carried out to evaluate the energy generated and consumed, considering a typical water mass of 450,000 t and a maximum gross pressure of 4.41 MPa. The results obtained in both analytical and numerical models show that unlike conventional pumped-storage hydropower plants, the round trip energy efficiency depends on the pressure inside the underground reservoir. The round trip energy efficiency could be reduced from 77.3% to 73.8% when the reservoir pressure reaches -100 kPa. In terms of energy balance, the energy generation decreases down to 3,639 MWh⁻¹ and the energy consumption increases up to 4,606 MWh year⁻¹ compared to optimal conditions.

1. Introduction

Renewable energy sources will have the fastest growth in the electricity sector, providing almost 30% of power demand in 2023, up from 24% in 2017 [1]. During this period, renewables are forecast to meet more than 70% of global electricity generation growth. Since, power generation varies continuously to meet demand fluctuations and ensure grid voltage and frequency stability, the improvement of electricity storage systems, such as Pumped Storage Hydropower (PSH), will be essential to ensure the grid integration of variable renewable energies (VRE) such as wind and solar photovoltaic, where the production depends on meteorological conditions and varies daily and seasonally. Moreover, when PSH is used to balancing, it also substitutes conventional fossil fuels (i.e. natural gas or coal), implying a reduction of greenhouse gas (GHG) emissions to the atmosphere. Francis pump-turbines are typically used to produce and consume electrical energy through an alternator-motor arrangement [2]. To adapt to the needs of the grid, modern PSH plants are equipped with variable-speed pump-turbine machines [3]. Wind-solar and PSH hybrid power supply system constitute a feasible option to achieve high penetration levels of VRE [4,5].

In the European Union (EU) there are approximately 270 PSH plants with a total generating capacity of 127 GW [6], representing 99% of the

electricity storage capacity [7,8]. Although there are some projects of Underground Pumped Storage Hydropower (UPSH) plants [9–17], nowadays there are not known plants under operation worldwide. The stored water in the upper reservoir (located at the surface) contains potential energy. When the electricity is needed, the water flows into the underground reservoir and runs a Francis turbine (generation mode) and the alternator, which feed electrical energy into the grid. Conversely, the energy from the electrical grid is used by the motor to run the Francis turbine in pumping mode (consumption), which drives the water from the underground reservoir (lower) to the surface reservoir (upper).

Unlike conventional PSH plants, where upper and lower reservoir are located at the surface, the operation of UPSH plants is complex due to the presence of water and air interacting during filling (generation) and emptying (pumping) processes. In an UPSH plant, the direction and the air flow rate depends on the operation mode and water flow rate, respectively. Menendez et al. [18] studied the effect of air pressure on the stability of the underground infrastructure (lower reservoir) during the operation time. To reduce the reservoir pressure, it is necessary to excavate air ducts between the underground reservoir and the surface (atmospheric conditions). An optimization of the global efficiency of UPSH plants could be achieved using this approach.

* Corresponding author.

E-mail address: jmenendezr@hunaser-energia.es (J. Menéndez).

In this work, the global operation, including both consumption and generation modes, in UPSH plants is analyzed. Turbine and pumping modes have been simulated with two Francis pump-turbines using disused mining structures in closed coal mines as lower reservoir. The energy balance (generation-consumption) and the round trip energy efficiency and how it varies depending on the pressure inside the lower reservoir is investigated. The main objective is to highlight the paramount importance of considering the reservoir pressure effects on the energy balance (generation and consumption), and therefore on economic results during the operation of a PSH plant with underground water reservoir.

2. Methodology

2.1. Problem statement

Conventional PSH are normally limited by topography restrictions. Disused underground space, such as closed coal mines or abandoned underground cavities, may be used as lower reservoir of UPSH plants. Thus, UPSH plants provide siting flexibility and retain the system reliability and availability characteristics of conventional PSH plants [19,20]. Moreover, the use of this type of underground structures has important environmental benefits compared to surface PSH plants (i.e. the excavation of large surface reservoirs) [12]. The energy generation and consumption in PSH plants depends on the water mass and the net head between upper and lower reservoirs. In the operation of UPSH plants the underground reservoir is at a different pressure from atmospheric pressure. In generation mode, the water flow displaces the existing air in the network of tunnels, which passes through the air ducts upwards. Conversely, in pumping mode, the water flow sucks the existing air in the outside atmosphere which passes through the air ducts downwards. Therefore, it is essential to analyze the reservoir pressure to know the behavior of UPSH plants during the operation time.

The round trip energy efficiency in surface PSH plants is calculated by dividing the energy output (turbine mode) by the energy input (pumping mode). The round trip energy efficiency takes values lower than 100% due to the losses, and usually it can vary in the 70–80% range [21–23]. A typical scheme of an UPSH plant using disused underground space (i.e. closed coal mines) is presented in Fig. 1. Maximum net head in

turbine mode (H_{NET-T}) and pumping mode (H_{NET-P}) are indicated. In a conventional PSH plant, the energy losses in penstock in turbine mode (h_{f-T}) and pumping mode (h_{f-P}), and the kinetic energy losses in the discharge into the lower reservoir (K_{e-T}) and upper reservoir (K_{e-P}) are considered to estimate the net head and the energy balance. As indicated in Fig. 1, to determine the net head in UPSH plants, it is also required to analyze the effect of the reservoir pressure during the operation time (h_p), in turbine mode (h_{p-T}) and pumping mode (h_{p-P}). The pressure inside the underground reservoir influences the energy balance and therefore the round trip energy efficiency. Finally, the round trip efficiency also includes the equipment-related losses (Francis pump-turbine, motor-generator and transformer) [24].

2.2. Francis turbines parameters and performance curves

Two Francis pump-turbines have been selected to analyze the influence of reservoir pressure on the round trip energy efficiency in UPSH plants. Table 1 shows the main parameters in pumping mode for Turbine 1 and Turbine 2. Table 2 shows the main parameters considered in turbine mode for the Turbine 1 and Turbine 2.

The non-dimensional performance curves for Francis Turbine 1 and Francis Turbine 2 are illustrated in Fig. 2 for both turbine and pumping operation modes, which correspond to typical situation encountered for Francis turbines in hydroelectric power plants. [25,26]. Two different scenarios have been analyzed in turbine mode, at 100% opening (full load) and at 40% opening (technical minimum). In pumping mode, only a scenario at full load has been considered, since the Francis turbine distributor is always opened at 100% in pumping mode [27,28].

2.3. Analytical model

Menendez et al. [26] carried out a similar study to analyze the effects of pressure inside the underground reservoirs of UPSH plants on the energy generation in turbine mode. As indicated in Fig. 1, the direction of air flow switches depending on the operation mode (turbine or pump). To study the operation of the Francis turbine in pumping mode and the evolution of the emptying phase, the previous 1-D analytical model developed in MATLAB and already validated in [26], has been reformulated for the reverse mode. The objective of the

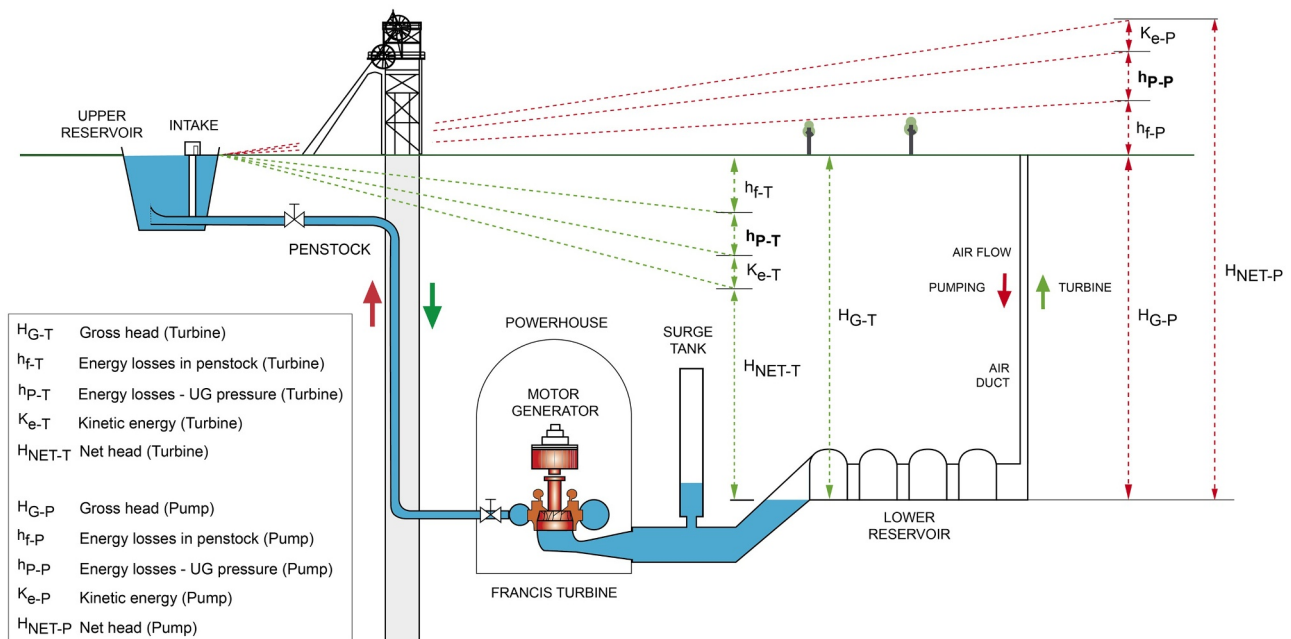


Fig. 1. Schematic design of an UPSH plant in closed mines. Energy lines in turbine and pumping modes. Influence of underground reservoir pressure on the energy generation and consumption (power output and power input).

Table 1
Main parameters considered in the study for Turbine 1 and Turbine 2 in pumping mode.

Pumping mode	Q (m ³ s ⁻¹)	Max. Gross Pressure (MPa)	Max. Net Pressure (MPa)	Min. Gross Pressure (MPa)	Min. Net Pressure (MPa)	Efficiency (%)	Max. Pump Input (MW)
Turbine 1	23	4.41	4.49	4.26	4.34	89.8%	114.86
Turbine 2	40	4.41	4.47	4.26	4.32	90.0%	199.76

Table 2
Main parameters considered in the study for Turbine 1 and Turbine 2 in turbine mode.

Turbine mode	Q (m ³ s ⁻¹)	Max. Gross Pressure (MPa)	Max. Net Pressure (MPa)	Min. Gross Pressure (MPa)	Min. Net Pressure (MPa)	Efficiency (%)	Max. Turbine Output (MW)
Turbine 1	32	4.41	4.27	4.26	4.12	91.4%	124.9
Turbine 2	55	4.41	4.30	4.26	4.15	91.4%	214.7

formulation is to estimate the values of the amount of energy consumed, the pressure inside the reservoir and the Mach number within the air ducts. Therefore, a system of equations is applied iteratively, with a time step of 1 s for water and for air between the maximum gross and minimum gross head. To solve the problem, the equations for the water circuit have been taken into account first. The energy equation between both reservoirs, together with the performance curve of the Francis turbines in pumping mode have been applied, see Eq. (1). In Eq. (2) mass conservation is applied to study the emptying of the lower reservoir and the filling of the upper one, considering a maximum gross pressure of 4.41 MPa and a minimum gross pressure of 4.26 MPa for a reservoir volume of 450,000 m³. For the air circuit, Eq. (3) has been applied to take into account that the pressure in the reservoir is a function of the overall head losses for the total air flow rate (which must be equal to the water flow of the pump according to continuity). In particular, the head losses are including both major losses and minor losses [29] which include, kinetic energy in the discharge to the upper reservoir, changes of direction and changes of cross-section. The major losses in the water and air circuit have been calculated using the equation formulated by D'arcy-Weisbach [30].

$$\frac{1}{\rho_w g} [aQ^2 + bQ + c] = h + K_1 Q^2 - \frac{P_{UG}}{\rho_w g} \quad (1)$$

$$\frac{dh}{dt} = m \frac{Q}{A} \quad m = 1 + \frac{H_{G \text{ MAX}} - H_{G \text{ MIN}} - H_T}{H_T} \quad (2)$$

$$\frac{P_{UG}}{\rho_a g} = \frac{-1}{\rho_a g} \frac{(K_2 + K_3 + K_4 + K_5)}{N^2} Q^2 \quad (3)$$

where:

- h = Gross pressure (MPa)
- K_1 = Loss coefficient (Major Losses, Water Flow)
- P_{UG} = Reservoir pressure (MPa)
- Q = Pump flow rate (m³ s⁻¹)
- $H_{G \text{ MAX}}$ = Maximum gross pressure (4.41 MPa)
- $H_{G \text{ MIN}}$ = Minimum gross pressure (4.26 MPa)
- H_T = Height of the tunnels (6.5 m)
- a, b and c = Coefficients of the pump equation
- A = Surface of the reservoir (m²)
- K_2 = Loss coefficient (Major Losses, Air Duct)
- K_3 = Loss for kinetic energy (Air Flow)
- K_4 = Loss for bends (Air Flow)
- K_5 = Loss for changes in cross -section (Air Flow)
- N = Number of air ducts
- g = Gravitational acceleration (9.81 m s⁻²)
- ρ_w = Water density (1000 kg m⁻³)
- ρ_a = Air density (1.2 kg m⁻³)

Geometrically, the one-dimensional analytical model considers a total water capacity of 450,000 m³ in an underground reservoir with the form of a network of connected tunnels with a cross-section of 30 m². Several design options based on the air input have been analyzed, from 1 to 6 air ducts with circular cross-section in the 0.2–4.68 m² range. The air ducts connect the reservoir with parts of the existing mining drifts through a 60 m long tube.

Due to the high velocities reached by the air flow in some of the cases analyzed, the model considered also the effects of compressible flow. To include this formulation in the model, the loss coefficient for compressible flow in pumping mode, K_{2c} , is defined according to

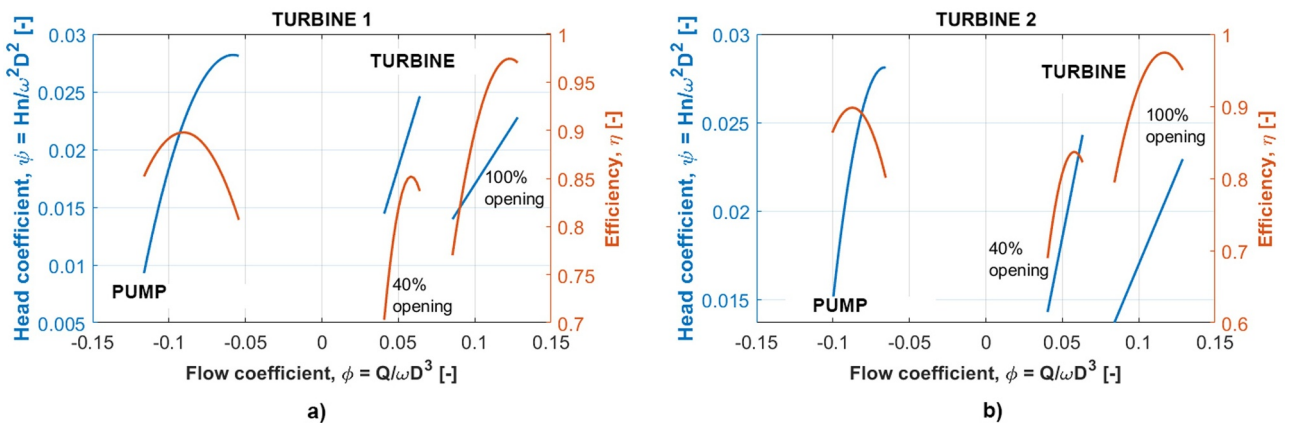


Fig. 2. Non-dimensional performance curves of the Francis turbines. (a) Turbine and pump performance curves for Francis Turbine 1 and; (b) Turbine and pump performance curves for Francis Turbine 2. Note: Typical diameters and rotational velocities have been employed for both Turbines (see [26]) to calculate the head and flow coefficients.

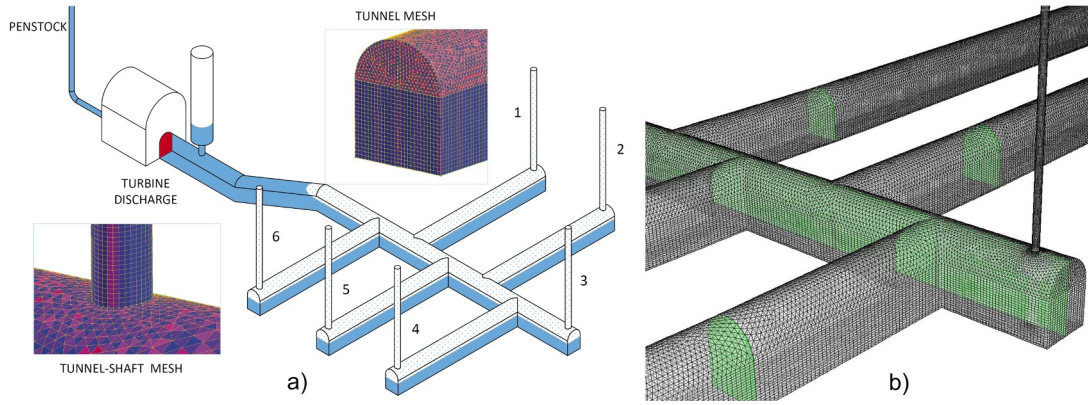


Fig. 3. CFD Numerical model. (a) 3D Geometry of the UPSH plant; (b) Mesh details of the model, tunnels and air duct.

Eq. (6). When the Mach number is higher than 0.3, the compressible flow calculation is activated, using this new coefficient in the system resolution. For that purpose, the formulation for the discharge of a pressurized gas tank through a long, narrow pipe has been adapted for the major loss in the air duct. In this case, it has been considered as a partial vacuum inside the reservoir that induces the suction of outside air at atmospheric conditions. Moreover, it has been assumed that the Mach number is below unity, with the convective term neglected and a maximum pressure inside the reservoir of 1 bar for practicability. Through Eq. (4) and Eq. (5) the pressure drop with compressible flow inside the reservoir is determined taking into account that the mass flow considered passes from the pressure in the outside atmosphere to the underground reservoir by means of air ducts, where the flow of air is sucked when the Francis pump turbine operates in pumping mode. The flow of water is equal to the sum of the air flow that comes in through air ducts. Because it is compressible flow, Eq. (6) determines the value of the major losses for a compressible flow K_{2c} , different from the coefficient K_2 that had been previously calculated.

$$\int_{P_{UG}}^{P_a} P_{UG} dp = \frac{P_{UG0}}{\rho_{a0}} \frac{f}{2DA_s^2} \dot{m}^2 \int_0^L dx \quad (4)$$

$$P_{UG} = P_a \frac{1}{\sqrt{1 + \frac{fL}{2D} \frac{\rho_{a0}}{P_0} (v)^2}} \quad (5)$$

$$K_{2c} = \frac{\left[1 - \frac{1}{\sqrt{1 - \frac{fL}{2D} \frac{\rho_{a0}}{P_{UG0}} v^2}} \right]}{Q^2} P_a \quad (6)$$

where:

- P_a = Atmospheric pressure (0.1013 MPa)
- f = Friction factor (0.02)
- A_s = Air duct section-cross (m^2)
- \dot{m} = Mass flow ($kg s^{-1}$)
- L = Air ducts length (60 m)
- Q = Flow rate ($m^3 s^{-1}$)
- D = Air ducts diameter (m)
- v = Air velocity ($m s^{-1}$)
- K_{2c} = Loss coefficient for compressible flow (Major Losses, Air Ducts)

2.4. CFD numerical models

To compare the results of the 1-D analytical model, a CFD numerical model has been carried out. Menendez et al. [26] already developed a 3D numerical model to investigate the effect of reservoir pressure on energy generation (turbine mode) in UPSH plants. For the present

investigation, the model has been modified to analyze the operation in pumping mode in order to evaluate the effect of reservoir pressure on energy consumption. Fig. 3 shows the geometry of the considered model and the mesh details. The objective of the simulation is to obtain the values of the water flow in the exit of the pump and reservoir pressures for different cross-sections of air duct, keeping constant the value of the maximum gross pressure at the entrance of the pump (4.41 MPa). Simulations were carried out with the turbines indicated in Table 1 and Table 2. The general design considers 6 ventilation shafts, one at the end of each tunnel. Simulations have been made for air ducts diameters of 0.5 m and 1 m. To economically optimize the design of the underground reservoir, calculations have also been made with a single shaft, located at the end of the central tunnel.

The simulations were performed with the commercial CFD software Ansys Fluent V16.0, solving the Unsteady Reynolds-Averaged Navier-Stokes (URANS) equations with a two-phase (water and air) scheme. This numerical model is developed meshing the geometry into different small cells in which the flow equations must be solved after discretization. In this model, a second-order upwind discretization has been implemented for convective terms, with a first order scheme for temporal terms and central differencing for diffusion terms. For the closure of turbulence, a robust k-epsilon RNG model with standard logarithmic wall functions was employed. The application of neutral boundary conditions has been fulfilled introducing large ventilation rooms where atmospheric pressure values were set on top, away from the vent shafts. Also, a porous jump (internal) boundary condition has been used to simulate the pump. For the water, a pressure outlet condition is imposed for the pump, representing the gross head that drives the water flow rate to the upper reservoir. Finally, the unsteady resolution of the discretized equations, with time steps in the order of 10^{-3} s, provides the final solution of the model. More precisely, variable time stepping was used in order to automatically change the time step when an interface is moving through finer meshes or if the interface velocity is high. The variable time step is based on the maximum Courant number near the VOF interface. A 3D structured mesh has been developed for the entire domain, employing tetrahedral and hexahedral cells because of their suitable adaptation to the geometry. The mesh used for the calculations reaches up to about 4.62×10^6 cells. More details for the mesh topology and the accuracy of the CFD model can be found in Menéndez et al. [26]. The Volume of Fluid (VOF) approach [31] has been selected for the two-phase (water and air) modeling.

3. Results and discussions

3.1. Analytical model results

The system of equations using MATLAB presented in Section 2.3 has been applied in order to know the evolution of the emptying of the

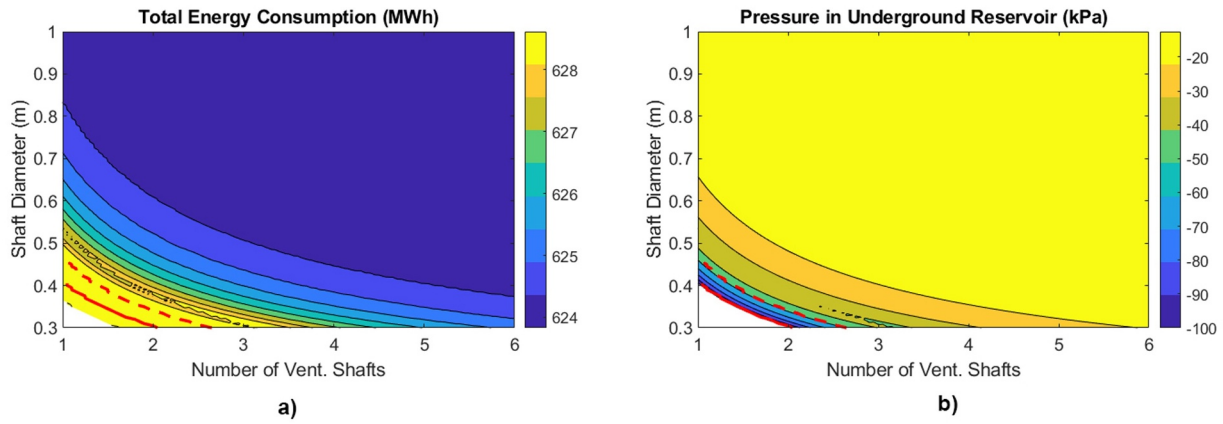


Fig. 4. Analytical model results for Turbine 1 in pumping mode depending on the air duct cross-section. Water flow rate at full load of $23 \text{ m}^3 \text{ s}^{-1}$. (a) Total energy consumption (MWh cycle^{-1}); (b) Negative relative pressure in underground reservoir (kPa).

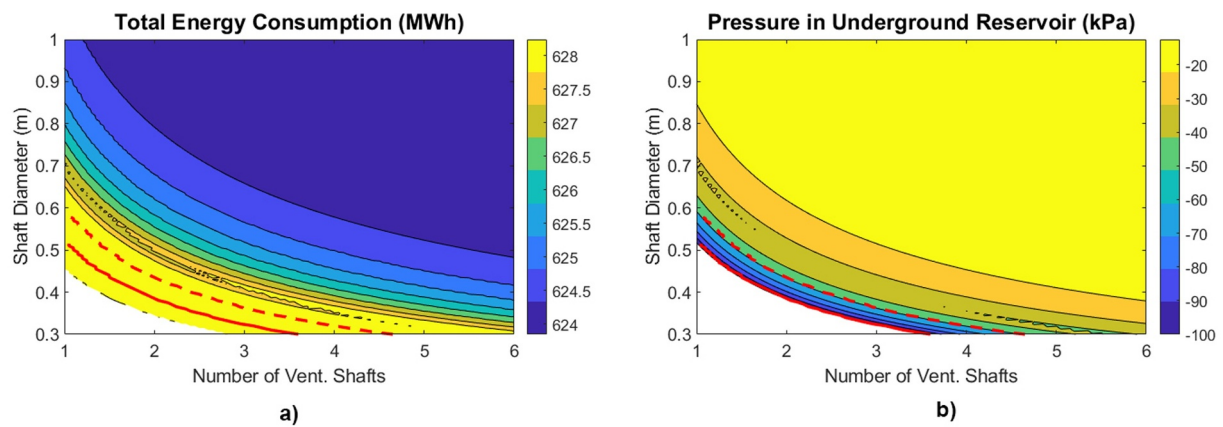


Fig. 5. Analytical model results for Turbine 2 in pumping mode depending on the air duct cross-section. Water flow rate at full load of $40 \text{ m}^3 \text{ s}^{-1}$. (a) Total energy consumption (MWh cycle^{-1}); (b) Negative relative pressure in underground reservoir (kPa).

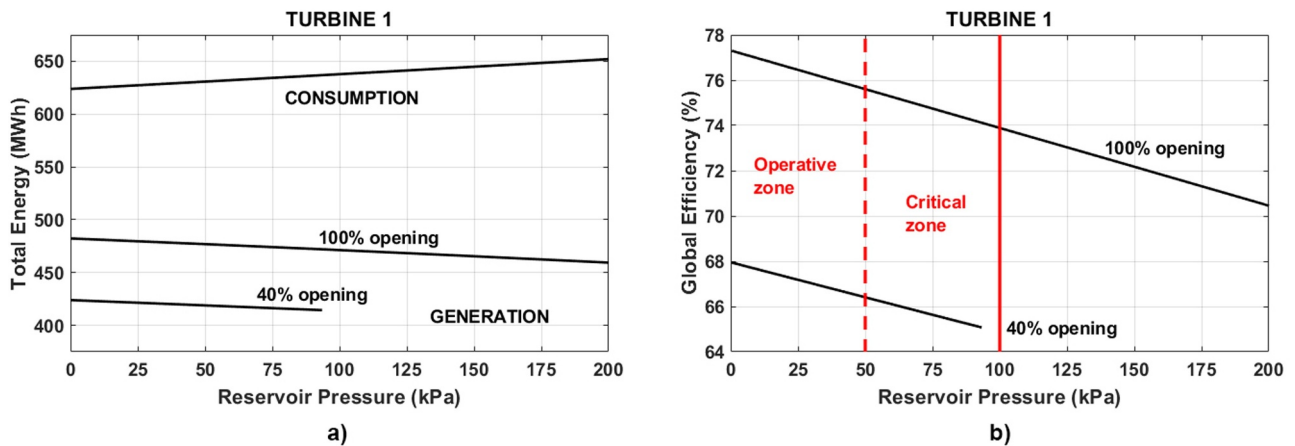


Fig. 6. Results for Turbine 1 considering a pressure in underground reservoir between 0–200 kPa. (a) Energy consumption and generation; (b) Round trip energy efficiency and feasible operating zones.

underground reservoir in pumping mode. Fig. 4 shows the results of the simulations for Turbine 1. A water flow rate of $23 \text{ m}^3 \text{ s}^{-1}$ between the maximum and minimum gross pressure (4.41 and 4.26 MPa, respectively) were considered. Fig. 4a shows the results for the total energy consumption (MWh cycle^{-1}) considering different cross-sections of air ducts. Fig. 4b shows the pressure in the underground reservoir (kPa). The pressure decreases when the air ducts cross-section decreases (higher values of negative relative pressure are required to aspirate the

outside air). The energy consumed reaches $623.83 \text{ MWh cycle}^{-1}$ when the pressure inside the lower reservoir is 0 kPa, and increases up to $637.79 \text{ MWh cycle}^{-1}$ when the reservoir pressure is 100 kPa. Fig. 4 also indicates different feasible operating zones with continuous and dashed red lines. The system would be in the compressible zone with non-negligible convective effects (extremely high velocities of air flow with shocked flow in the air ducts) if the cross-section of air ducts is lower than 0.13 m^2 . Note that isolines of cross-section correspond to

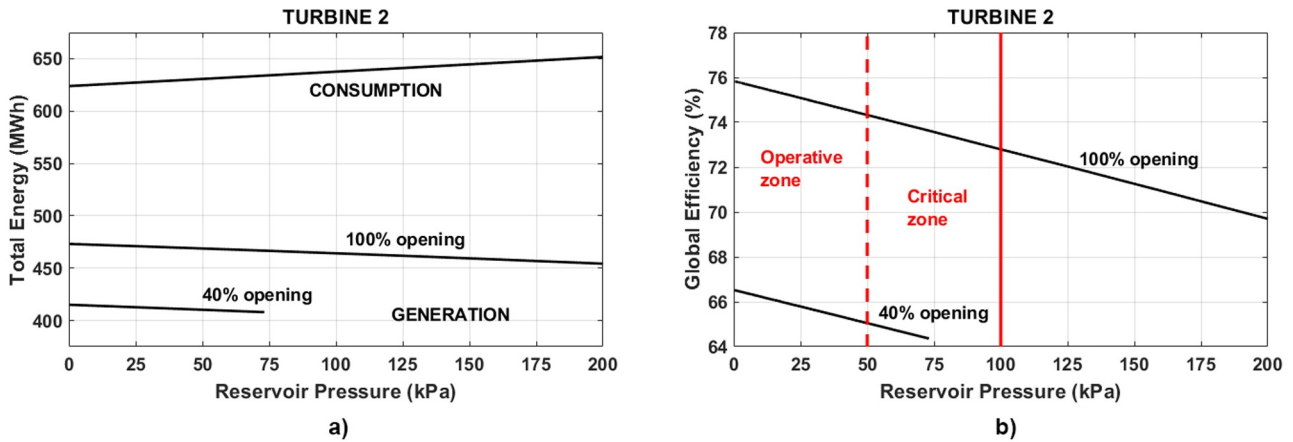


Fig. 7. Results for Turbine 2 considering a pressure in underground reservoir between 0–200 kPa. (a) Energy consumption and generation; (b) Round trip energy efficiency and feasible zones of operation.

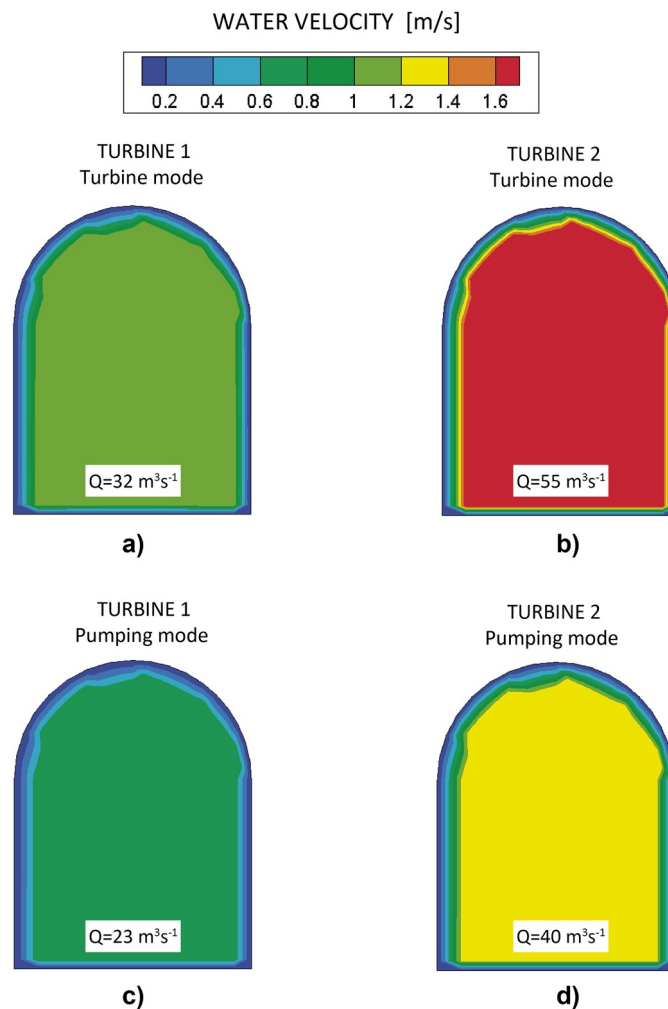


Fig. 8. Numerical simulations results. Water velocity and flow rate in the tunnels of underground reservoir during operation phase. (a) Turbine 1 in turbine mode; (b) Turbine 2 in turbine mode; (c) Turbine 1 in pumping mode and; (d) Turbine 2 in pumping mode.

hyperbolas in the plots. When the cross-section is between 0.12–0.2 m² the system would be in a compressible zone but with negligible convective effects. Therefore, it is recommended to operate with a reservoir pressure higher than –50 kPa (cross-section of air ducts greater than 0.2 m²).

Similar results are obtained for Turbine 2 and illustrated in Fig. 5. A

water flow rate of 40 m³ s⁻¹ in pumping mode at full load and the same gross head as for Turbine 1 have been considered. In this model, the compressible zone with non-negligible convective effects is reached for cross-section of air duct lower than 0.2 m². When the cross-section of air duct is between 0.2–0.28 m² the system would be in compressible zone with negligible convective effects. For Turbine 2, it is also

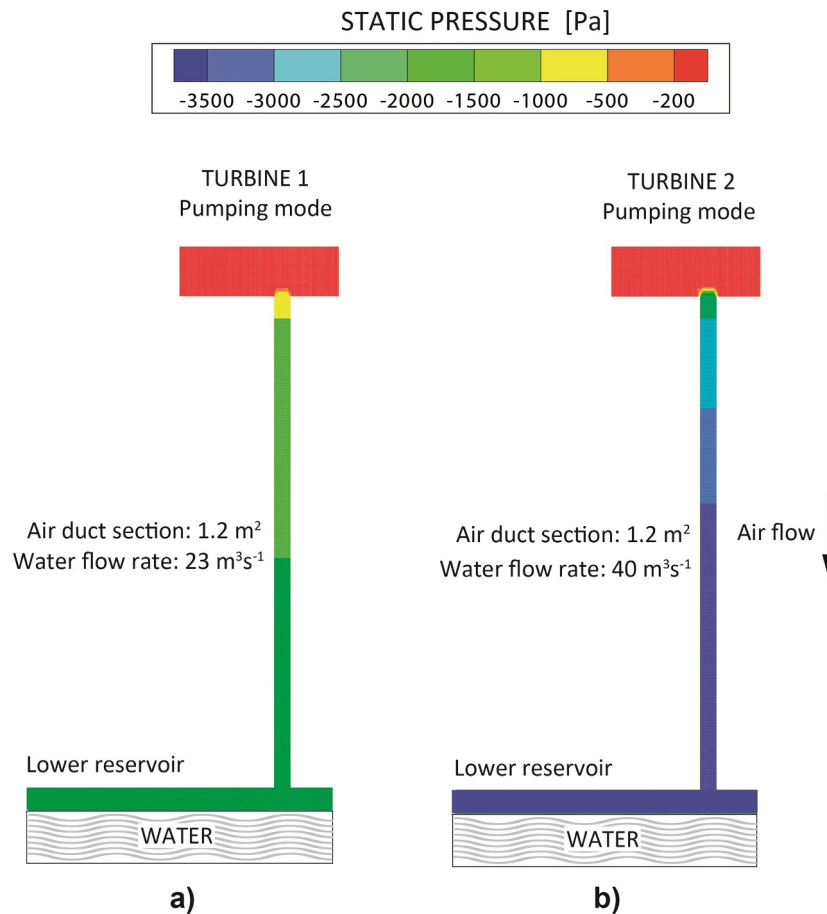


Fig. 9. Static pressure in the lower reservoir and air duct in pumping mode. Reservoir partially filled with water. (a) Turbine 1 with an air duct cross-section of 1.2 m^2 ; (b) Turbine 2 with a cross-section of air ducts of 1.2 m^2 .

recommended to operate outside the compressible zone, with air duct cross-section greater than 0.4 m^2 and reservoir pressure higher than -50 kPa .

In Fig. 6, the results obtained by Menendez et al. [26] in generation mode at 100% opening (full load) and at 40% opening (technical minimum), have been combined with the simulations in pumping mode to obtain the round trip energy efficiency of the UPSH plant. Fig. 6a shows the energy generation and consumption for the Turbine 1 considering a reservoir pressure in the $0\text{--}200 \text{ kPa}$ range. Here, it must be noticed that negative relative pressures in the pumping mode have been represented as positive values for convenience, in order to ease the comparison. The energy generation decreases and the energy consumption increases when the reservoir pressure increases. Specifically, in the pressure range considered, the energy generation decreases from 482.27 to $455.78 \text{ MWh cycle}^{-1}$, and the energy consumption increases from 623.83 to $650 \text{ MWh cycle}^{-1}$. Fig. 6b shows the round trip energy efficiency for the same pressure range. Fig. 6b also indicates different operating zones, coinciding with the zones indicated in Fig. 4 (continuous and dashed red lines). In the feasible operating zones, the global efficiency varies from 77.3% at a pressure of 0 kPa to 73.8% when the reservoir pressure reaches -100 kPa . If the pressure is reduced to -50 kPa (upper limit of the recommended operating zone), the global efficiency results 75.6% .

Following, the results obtained for Turbine 2 are shown in Fig. 7. Once again, the pressure in the underground reservoir is considered as positive in both situations (turbine and pumping modes). Operative zones are also indicated in Fig. 7b with continuous and dashed red lines, as indicated for this model in Fig. 5. The energy generation decreases from 473.08 to $452.30 \text{ MWh cycle}^{-1}$ and the energy

consumption increases from 623.83 to $650 \text{ MWh cycle}^{-1}$ in the pressure range of $0\text{--}200 \text{ kPa}$. Within feasible operating zones, the round trip energy efficiency varies from 75.8% to 72.7% when the reservoir pressure is in the $0\text{--}100 \text{ kPa}$ range. If the air duct cross-section is designed to reach a reservoir pressure of 50 kPa , the global efficiency increases up to 74.3% . Finally, when the reservoir pressure reaches values of 25 kPa , the global efficiency would be of 75.1% . In generation mode, operating at 40% load ($12.8 \text{ m}^3 \text{ s}^{-1}$ and $22 \text{ m}^3 \text{ s}^{-1}$ of water flow rate for Turbine 1 and Turbine 2, respectively), the operation pressure in the reservoir reaches lower values, although the global efficiency is also penalized.

Although it is recommended to operate at reservoir pressures lower than 50 kPa in both Turbine 1 and Turbine 2, outside the compressible zone to avoid extremely high velocities and shocked conditions in the air ducts, the generation of energy is maximized and energy consumption is minimized when the cross-section of the air ducts is greater than 4 m^2 (equivalent to single air duct with 2.25 m in diameter).

3.2. Numerical model results

The CFD simulations that have been carried out for the present investigation analyze the main fluid-dynamic parameters (static pressure and water velocities in the underground reservoir and static pressure and air velocities in the air ducts) during the emptying of the underground water reservoir. The simulations have been performed with the reservoir partially filled with water. The model considers the performance curves shown in Fig. 2 for both Turbine 1 and Turbine 2 as an internal boundary condition and a pressure outlet of 4.41 MPa equivalent to the maximum gross head at the entrance of the Francis

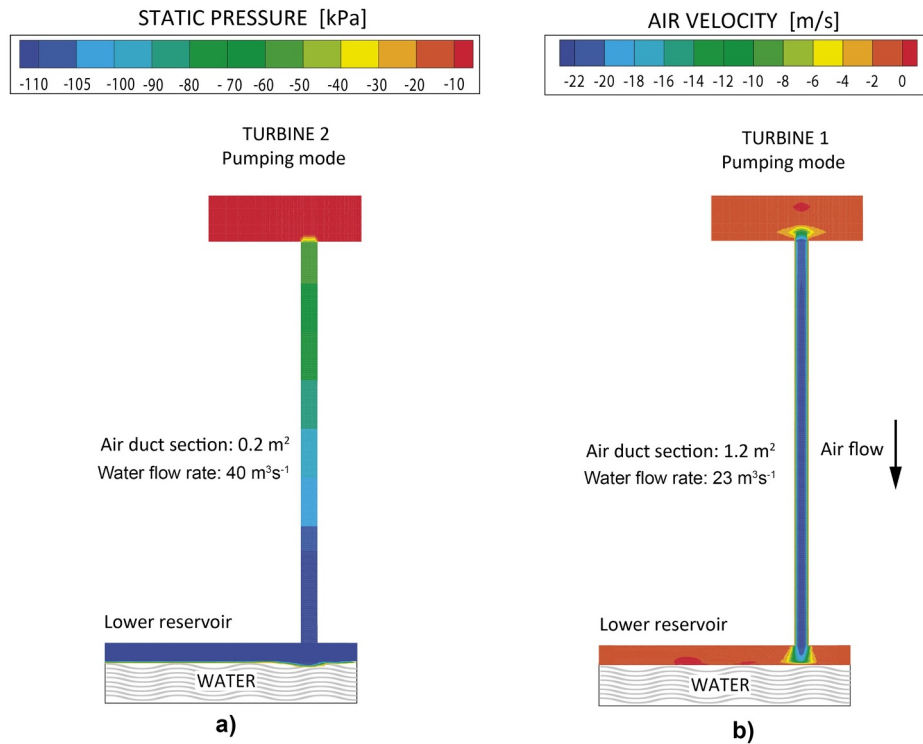


Fig. 10. (a) Static pressure in the lower reservoir of Turbine 2 in pumping mode and an air duct cross-section of 0.2 m²; (b) Air velocity in the air duct and lower reservoir for Turbine 1 in pumping mode and an air duct cross-section of 1.2 m².

turbines. The simulations have been developed for different air duct cross-section (0.2–1.2 m²) and the simulation time has been extended until the transient evolution of the initial stage is fulfilled. Fig. 8 shows the water flow velocities at the entrance of the Francis turbines (completely submerged) in the lower reservoir for both generation and consumption modes. The water flow rate has been verified in the simulations for Turbine 1 and Turbine 2, and the results obtained match the design parameters of the turbines that have been considered.

Fig. 9 shows the static pressure in the underground reservoir for Turbine 1 (Fig. 9a) and Turbine 2 (Fig. 9b) during the operation of the UPSH plant in pumping mode. A cross-section of air ducts of 1.2 m² has been considered. The water flow rate in Turbine 2 (40 m³ s⁻¹) is greater than the water flow rate in Turbine 1 (23 m³ s⁻¹). The static pressure in the reservoir reaches -1.56 kPa for Turbine 1 and -3.65 kPa for Turbine 2.

Complementarily, Fig. 10a shows the static pressure for Turbine 2 considering an air ducts cross-section of 0.2 m². The air velocity in underground reservoir and air duct is shown for Turbine 1 in Fig. 10b considering an air duct cross-section of 1.2 m² and a water flow rate of 23 m³ s⁻¹.

When the air ducts cross-section is reduced up to 0.2 m², the static pressure in the lower reservoir for Turbine 2 exceeds the operating limit (-100 kPa). Regarding the static pressure in the same Turbine 2 with a cross-section of air ducts of 1.2 m², the pressure increases strongly up to -3.65 kPa. The maximum air flow velocity reaches -22 m s⁻¹ in the

air duct, and this value decreases in the reservoir. Water and air flows are interacting during the emptying process. In both Figs. 9 and 10, the depth of the water sheet inside the reservoir can be seen. The gap between the water sheet and the roof of the reservoir is occupied by air.

3.3. Comparison between analytical and numerical results

The results obtained in both analytical and CFD numerical models are compared in Table 3. Reservoir pressure values in Turbine 1 and Turbine 2 considering air ducts cross-section of 0.2 and 1.2 m² are shown in pumping mode. Both analytical and CFD numerical models present similar results. The biggest difference (around a 14% discrepancy) is observed in Turbine 1 with an air duct cross-section of 0.2 m², varying from -1.34 to -1.56 kPa.

3.4. Assessment of energy losses and economic impact

Considering a water mass of 450,000 t and a maximum gross pressure of 4.41 MPa the energy generation is 159 and 156 GWh year⁻¹ for Turbine 1 and Turbine 2, respectively. The operation pressure in the underground reservoir influences the energy balance and therefore, it has an important impact on the economic results. Energy balance and economic impacts regarding optimal conditions are shown in Fig. 11. Fig. 11a shows the reduction in energy generation and the increase in energy consumption for Turbine 1 and Turbine 2 when the operation

Table 3
Comparison between the results obtained in analytical and numerical models for Turbine 1 and Turbine 2.

Turbine	Water flow rate (m ³ s ⁻¹)	Air duct section (m ²)	Reservoir pressure (kPa) Analytical models	Reservoir pressure (kPa) Numerical models
Turbine 1	23	0.2	-33.76	-36.79
		1.2	-1.34	-1.56
Turbine 2	40	0.2	-107.80	-114.00
		1.2	-3.58	-3.65

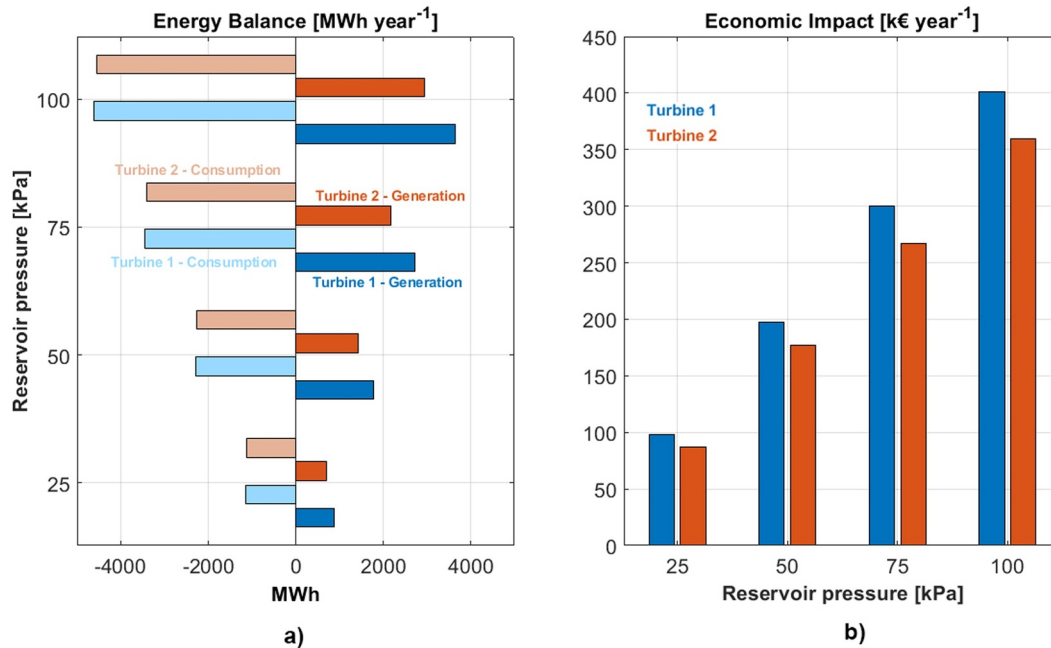


Fig. 11. (a) Energy balance in Turbine 1 and Turbine 2 with operation pressure values between 25–100 kPa (energy generation and consumption); (b) Economic impact in k€ year⁻¹.

pressure (in absolute values) varies from 25 to 100 kPa. Fig. 11b shows the economic impact considering an average price in the daily market of 56.31 € MWh⁻¹ for energy generation (turbine mode) and a cost of 42.56 € MWh⁻¹ for energy consumption (pumping mode) [[26],[32]]. When the pressure inside the lower reservoir reaches 100 kPa, an increase in energy consumption of 4606.80 MWh year⁻¹ in Turbine 1 and 4550.70 MWh year⁻¹ in Turbine 2, is produced. Regarding the energy generation at -100 kPa, it is reduced to 3639.90 MWh year⁻¹ for Turbine 1 and to 2950.20 MWh year⁻¹ for Turbine 2. From the economic point of view, when the reservoir pressure reaches -100 kPa, it has an impact of 401.03 k€ year⁻¹ for Turbine 1 and 359.80 k€ year⁻¹ for Turbine 2.

4. Conclusions

In this paper, the round trip energy efficiency of UPSH plants has been investigated. In addition, an optimization of the global efficiency in UPSH plants has been envisaged using this approach. Two Francis pump-turbines with a power output of 124.9 and 214.7 MW (turbine) and a power input of 114.8 and 199.7 MW (pump), have been selected. Unlike conventional PSH plants, where both upper and lower reservoir are located at the surface, the round trip energy efficiency of UPSH plants depends on the operation pressure in the underground water reservoir. Analytical and CFD numerical models have been developed to analyze the pressure inside the reservoir during the operation of UPSH plants. The reservoir pressure depends on the water flow rate in both turbine and pumping modes and the cross-section of air ducts. The reservoir pressure has a negative effect on the energy balance (generation-consumption) and economic results. A water mass of 450,000 t and a gross pressure of 4.41 MPa have been considered in both analytical and numerical simulations.

The results obtained for the pumping mode show that it is recommended to operate at least with reservoir pressures higher than -50 kPa, outside the compressible zone to avoid high velocities of air flow and shocked conditions in the air ducts. For Turbine 1, when the operation pressure reaches -100 kPa an increase in energy consumption up to 4606.80 MWh year⁻¹ and a reduction down to 3639.90 MWh year⁻¹ in energy generation may be produced. This

implies a reduction in the round trip energy efficiency from 77.3% to 73.8%. Economically, it means accumulated losses of 401.03 k€ year⁻¹ compared to optimal conditions. For Turbine 2, the round trip energy efficiency varies from 75.8% to 72.7% and the economic losses reach 359.80 k€ year⁻¹ when the reservoir pressure varies from 0 to -100 kPa. In summary, an impact on the energy balance of 8246.7 and 7500.9 MWh year⁻¹ is produced at an operation pressure of -100 kPa for Turbine 1 and Turbine 2, respectively. Although it is recommended to operate at reservoir pressures higher than -50 kPa in both Turbine 1 and Turbine 2 (outside the compressible zone), the generation of energy is maximized and energy consumption is minimized when the cross-section of the air ducts is greater than 4 m².

CRedit authorship contribution statement

Javier Menéndez: Conceptualization, Software, Data curation, Visualization, Writing - original draft. **Jesús M. Fernández-Oro:** Methodology, Writing - review & editing, Validation. **Mónica Galdo:** Methodology, Formal analysis, Software. **Jorge Loredo:** Supervision.

Declaration of Competing Interest

The authors declare that they have no known competing financial interests or personal relationships that could have appeared to influence the work reported in this paper.

References

- [1] International Energy Agency (IEA). Key world energy trends, except from: renewables information.
- [2] R Tao, X Zhou, B Xu, Z Wang, Numerical investigation of the flow regime and cavitation in the vanes of reversible pump-turbine during pump mode's starting up, *Renew. Energy* 141 (2019) 9–19, <https://doi.org/10.1016/j.renene.2019.03.108>.
- [3] I Iliev, C Trivedi, OG Dahlhaug, Variable-speed operation of Francis turbines: A review of the perspectives and challenges, *Renew and Sust. Energy Rev.* 103 (2019) 109–121, <https://doi.org/10.1016/j.rser.2018.12.033>.
- [4] AA Salimi, A Karimi, Y Noorzadeh, Simultaneous operation of wind and pumped storage hydropower plants in a linearized security-constrained unit commitment model for high wind energy penetration, *J. Energy Storage* 22 (2019) 318–330, <https://doi.org/10.1016/j.est.2019.02.026>.
- [5] FA Canales, A Beluco, C Mendes, A comparative study of a wind hydro hybrid system with water storage capacity: Conventional reservoir or pumped storage

- plant? *J. Energy Storage* 4 (2015) 96–105, <https://doi.org/10.1016/j.est.2015.09.007>.
- [6] M Manwaring, D Mursch, K Tilford, Challenges and Opportunities For New Pumped Storage Development, National Hydropower Association, 2012 Technical Report.
- [7] C Doetsch, A Kanngiesser, D Wolf, Speicherung elektrischer Energie – Technologie zur Netzintegration erneuerbarer Energien, *uwf UmweltWirtschaftsForum* 17 (4) (2009) 351–360, <https://doi.org/10.1007/s00550-009-0150-3>.
- [8] S Rehman, LM Al-Hadhrani, MM Alam, Pumped hydro energy storage system: a technological review, *Renew. Sustain. Energy Rev.* 44 (2015) 586–598, <https://doi.org/10.1016/j.rser.2014.12.040>.
- [9] R Alvarado, A Niemann, T Wortberg, Underground pumped-storage hydroelectricity using existing coal mining infrastructure, *E-Proceedings of the 36th IAHR World Congress*, 28 June–3 July, 2015, The Netherlands: The Hague, 2015.
- [10] J. Menendez, J. Loredó, J.M. Fernández-Oro, M. Galdo, Energy storage in underground coal mines in NW Spain: assessment of an underground lower water reservoir and preliminary energy balance, *Renew. Energy* 134 (2019) 1381–1391, <https://doi.org/10.1016/j.renene.2018.09.042>.
- [11] Madlener R, Specht JM. 2013. An exploratory economic analysis of underground pumped-storage hydro power plants in abandoned coal mines. FCN Working Paper No. 2/2013.
- [12] IH. Wong, An underground pumped storage scheme in the bukit Timah granite of Singapore, *Tunn. Undergr. Space Technol.* 11 (4) (1996) 485–489.
- [13] G. Isaaksson, D. Nilsson, T. Sjostrand, Pumped storage power plants with underground lower reservoirs, *Seventh World Power Conference, Section 2, Paper 160*, Moscow, 1968.
- [14] N. Uddin, Preliminary design of an underground reservoir for pumped storage, *Geotech. Geol. Eng.* 21 (2003) 331–355, <https://doi.org/10.1023/B:GEGE.0000006058.79137.e2>.
- [15] J. Menendez, A. Ordoñez, R. Alvarez, J. Loredó, Energy from closed mines: underground energy storage and geothermal applications, *Renew. Sustain. Energy Rev.* 108 (2019) 498e512, <https://doi.org/10.1016/j.rser.2019.04.007>.
- [16] F Winde, F Kaiser, E Erasmus, Exploring the use of deep level gold mines in South Africa for underground pumped hydroelectric energy storage schemes, *Renew. Sustain. Energy Rev.* 78 (2016) 668–682, <https://doi.org/10.1016/j.rser.2017.04.116>.
- [17] E Pujades, P Orban, S Bodeux, P Archambeau, S Ercicum, A Dassargues, Underground pumped storage hydropower plants using open pit mines: how do groundwater exchanges influence the efficiency? *Appl. Energy* 190 (2017) 135–146, <https://doi.org/10.1016/j.apenergy.2016.12.093>.
- [18] J Menéndez, F Schmidt, H Konietzky, J.M Fernández-Oro, M Galdo, J Loredó, M.B Díaz-Aguado, Stability analysis of the underground infrastructure for pumped storage hydropower plants in closed coal mines, *Tunn. Undergr. Space Technol.* 94 (2019) 103117, <https://doi.org/10.1016/j.tust.2019.103117>.
- [19] S.W. Tam, C.A. Blomquist, G.T. Kartsounes, Underground pumped hydro storage—an overview, *Energy Sources* 4 (4) (1979) 329–351.
- [20] CR Matos, JF Carneiro, PP Silva, Overview of large-scale underground energy storage technologies for integration of renewable energies and criteria for reservoir identification, *J. Energy storage.* 21 (2019) 241–258, <https://doi.org/10.1016/j.est.2018.11.023>.
- [21] SM Schoenung, JM Eyer, JJ Iannucci, SA Horgan, Energy Storage for a competitive power market, *Annu. Rev. Energy Environ.* 21 (1) (1996) 347–370, <https://doi.org/10.1146/annurev.energy.21.1.347>.
- [22] H Ibrahim, A Ilinca, J Perron, Energy storage systems: characteristics and comparisons, *Renew. Sustain. Energy Rev.* 12 (5) (2008) 1221–1250, <https://doi.org/10.1016/j.rser.2007.01.023>.
- [23] C-J Yang, RB Jackson, Opportunities and barriers to pumped-hydro energy storage in the United States, *Renew. Sustain Energy Rev.* 15 (1) (2011) 839–844, <https://doi.org/10.1016/j.rser.2010.09.020>.
- [24] MWH Americas, Technical analysis of pumped storage and integration with wind power in the Pacific northwest, U.S. Army corps of engineers hydroelectric design center, 2009 Technical Report.
- [25] Rahul Goyal, Bhupendra K. Gandhi, Review of hydrodynamics instabilities in Francis turbine during off-design and transient operations, *Renew. Energy* 116 (Part A) (2018) 697–709.
- [26] J. Menendez, J.M. Fernández-Oro, M. Galdo, J. Loredó, Pumped-storage hydro-power plants with underground reservoir: influence of air pressure on the efficiency of the Francis turbine and energy production, *Renew. Energy.* 143 (2019) 1427–1438, <https://doi.org/10.1016/j.renene.2019.05.099>.
- [27] J.M. Blanco, J.C. Saenz-Díez, E. Jimenez, M. Perez de la Parte, Comparison in the application of the exploitation by optimal head model to hydroelectric power stations in run-of-the-river systems equipped with different types of turbines, *RE&PQJ* 1 (2011) 1338–1343, <https://doi.org/10.24084/repqj09.643>.
- [28] J. Schmidt, W. Kemmetmüller, A. Kugi, Modeling and static optimization of a variable speed pumped storage power plant, *Renew. Energy* 111 (2017) 38–51, <https://doi.org/10.1016/j.renene.2017.03.055>.
- [29] *Subsurface Ventilation and Environmental Engineering*, J Malcolm, McPherson, Chapman & Hall, 2009, p. 824.
- [30] Frank M White, *Fluid Mechanics*, Seventh ed., (2011), p. 861.
- [31] C. Hirt, B. Nichols, Volume of fluid (VOF) method for the dynamics of free boundaries, *J. Comput. Phys.* 39 (1981) 201–225, [https://doi.org/10.1016/0021-9991\(81\)90145-5](https://doi.org/10.1016/0021-9991(81)90145-5).
- [32] Iberian Energy Market Operator. OMIE, 2019. www.omie.es (Accessed 17 September 2019).